The effect of receiver antenna array horizontal orientation on MIMO channel capacity

Almers, Peter; Tufvesson, Fredrik; Karlsson, P; Molisch, Andreas

Published in:
[Host publication title missing]

DOI:
10.1109/VETECS.2003.1207496

2003

The Effect of Horizontal Array Orientation on MIMO Channel Capacity

Peter Almers[1,2], Fredrik Tufvesson[2], Peter Karlsson[1] and Andreas F. Molisch[2,3]

[1]Telia Research AB, Box 94, SE-201 20 Malmö, Sweden
[2]Dept. of Electroscience, Lund University, Box 118, SE-221 00 Lund, Sweden
[3]Mitsubishi Electric Research Lab, 558 Central Avenue, Murray Hill, NJ 07974, USA
E-mail: Peter.Almers@es.lth.se

***Abstract*— In multiple-input multiple-output (MIMO) systems the horizontal orientation of a linear array has, in some situations, a large influence on the available channel capacity. In this paper we investigate the effect of horizontal array orientation on channel capacity, eigenvalue distribution and antenna complex correlation coefficient in such systems. We present channel measurements in an office corridor environment for a 6 $\times$ 6 MIMO system and compare the capacity results to those of a physical and non-physical model based on the measurements. The results show that under LOS conditions the channel capacity can vary significantly depending on the receiver array orientation in the horizontal plane.**

I. Introduction

Large capacity gains in wireless systems can be achieved by using multiple antennas at the receiver and the transmitter [1] [2] [3]. These so called multiple-input multiple-output (MIMO) systems are therefore of great interest to the wireless industry. During the recent years, numerous investigations of the channel capacity have been performed to find out how the capacity is affected by, e.g., antenna correlation [4], antenna configuration [5], array size, etc. Measurement campaigns have been carried out to verify the theoretical results and to find realistic MIMO channel models [6] [7] [8]. The effects of the *vertical* array orientation on channel capacity has been studied for different indoor propagation environments in [9], where the corresponding antenna correlation coefficients were presented.

In this paper we study the effect on the capacity when the receiving array is rotated in the *horizontal* plane. The differences in the capacity are measured in an indoor corridor environment with a center frequency of 5.475 GHz. We investigate the eigenvalue distribution and the antenna correlation coefficient for the different orientations to explain the differences in capacity. The measured capacities are also compared to results from a physical model derived from estimated direction of arrival (DOA) and direction of departure (DOD), and a statistical model based on the measured antenna correlations.

The paper is arranged as follows: In Section II the measurement setup is described. Next, in Section III, we review some aspects of the channel capacity and its derivation from measured channel transfer function matrices, and describe the capacity results we obtained in our measurement. In Section IV we then study the DOA and DOD. Finally, in Section V, we compare the measurements results with the two models and present the conclusions in Section VI.

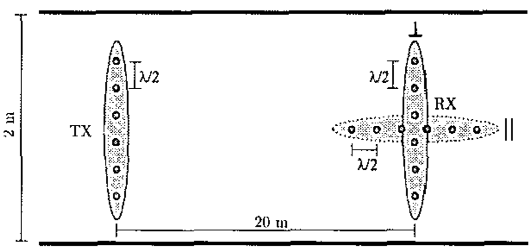

Fig. 1. Antenna measurement setup showing the receiver array setup parallel to the LOS (||), and the receiver array setup perpendicular to the LOS (⊥).

II. MIMO Channel Measurements

The measurements are performed with a vector network analyzer (Rohde & Schwartz ZVC) and virtual arrays at both transmitter and receiver. The environment in which the antennas are located is a 100 m long and 2 m wide corridor with concrete walls and offices lined up on both sides, see Fig. 1. For each transmit antenna position, the complex transfer functions were recorded for 12 receive antenna positions, 6 positions with the broadside of the virtual antenna parallel to the LOS and 6 positions with the broadside perpendicular to the LOS. 201 frequency points were measured in the frequency band 5.225 – 5.725 GHz. The measured signal-to-noise ratio (SNR) was estimated to 19 dB. The transmitter and the receiver antenna elements of the two synthetic arrays are omnidirectional wideband conical antennas with a separation of half a wavelength.

The distance between the transmitter and the receiver was 20 m. Measurements were conducted out of office hours in order to minimize effects of external disturbances to the channel.

III. CHANNEL CAPACITY

A. Theory

In the paper we consider the capacity for a single link in a flat-fading channel. The input-output relation of the MIMO system is described by

$$\mathbf{r} = \mathbf{H}\mathbf{s} + \mathbf{n}, \tag{1}$$

where $\mathbf{r} = [r_1 \cdots r_{N_\mathrm{R}}]^T$ is the received signal vector, $\mathbf{s} = [s_1 \cdots s_{N_\mathrm{T}}]^T$ is the corresponding transmitted signal vector with mean power $E\left[\mathbf{s}\mathbf{s}^\dagger\right] = P/N_\mathrm{T}$, where $(\cdot)^\dagger$ represents conjugate transpose, P is the total transmit power, N_R and N_T is the number of receive and transmit antenna elements respectively, and finally $\mathbf{n}$ is a vector whose entries are complex uncorrelated white Gaussian noise samples with variance σ^2. If the transfer matrix, $\mathbf{H}$, is known at the transmitter and receiver side it can be transformed into a number of independent Gaussian channels referred to as *eigenmode channels* [3]. $\mathbf{H}$ is normalized as $E\left[\|\mathbf{H}\|_F^2\right] = N_\mathrm{R} N_\mathrm{T}$. The power gains of the eigenmode channels are given by the eigenvalues λ_k of the correlation matrix $\mathbf{H}\mathbf{H}^\dagger$

$$\begin{array}{ll} \mathbf{H}\mathbf{H}^\dagger = \mathbf{U}\mathbf{\Lambda}\mathbf{U}^\dagger, & N_\mathrm{R} < N_\mathrm{T} \\ \mathbf{H}^\dagger\mathbf{H} = \mathbf{V}\mathbf{\Lambda}\mathbf{V}^\dagger, & N_\mathrm{R} \geq N_\mathrm{T} \end{array}, \tag{2}$$

where $\mathbf{U}$ and $\mathbf{V}$ are a unitary matrices, $\mathbf{\Lambda}$ is a diagonal matrix containing K eigenvalues λ_k. These eigenvalues are equal to the squared magnitude of the singular values of $\mathbf{H}$. The number of eigenmode channels K depends of the number of resolvable multipath components (MPC), L, and the number of antenna elements at the receiver and the transmitter ($K \leq L$).

In order to evaluate the performance of different receiver array directions, we use the normalized channel capacity (in bits/s/Hz). For the k :th eigenmode channel it can be expressed as [10]

$$C_k = \log_2\left(1 + \frac{p_k \lambda_k}{\sigma^2}\right), \tag{3}$$

where p_k denotes the power transmitted on the λ_k eigenmode channel, and σ^2 is the power of the white Gaussian noise. The total normalized MIMO channel capacity for a flat fading MIMO channel is then

$$C = \sum_{k=1}^{K} \log_2\left(1 + \frac{p_k \lambda_k}{\sigma^2}\right). \tag{4}$$

The channel capacity depends on the power allocation between the eigenmode channels. In this paper, uniform power allocation is considered, i.e., $p_k = \frac{P}{K}$. Additional capacity gains from waterfilling is evaluated in [11], and not considered in this paper.

B. Capacity measurement results

We calculate the capacity for the different channel realizations using the measured transfer function matrices. In Fig. 2 the mean capacities for different array sizes ($N_\mathrm{R} = N_\mathrm{T}$) is shown. Due to the estimated measured SNR of 19 dB, the capacities are evaluated at a smaller SNR, namely 15 dB. For comparison purposes the capacities for an independent identically distributed (i.i.d.) Gaussian channel, and the capacity for a pure, non-scattering, LOS channel are also plotted.

From this plot, we can make the following observations:

- As expected, the presence of strong LOS results in a capacity gain that is lower than that of the i.i.d. Gaussian channel [12].
- The capacity increases linearly with the number of antenna elements, indicating that there is a sufficient number of strong MPCs providing independent transmission paths for different data streams.
- We measure a significant difference between the capacities achieved by parallel and perpendicular arrays. The perpendicular array results in a higher capacity gain than the parallel array. We conclude that for deterministic channels, with a strong LOS and small angular spread, the horizontal orientation of the receiver antenna array can make a significant difference in the channel capacity gain. The possible reasons for this observation will be discussed in the next section.

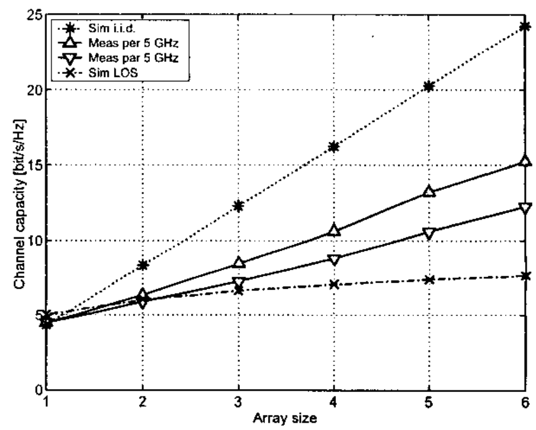

Fig. 2. Mean capacity for different array sizes ($N_\mathrm{R} = N_\mathrm{T}$) evaluated at a SNR of 15 dB.

It is also interesting to study the eigenvalues of the channel matrix, as it totally describes the channel capacity. In Fig. 3 we plot the mean of the ordered eigenvalues of the i.i.d. channel, and of the parallel and perpendicular orientation of the measured channel. It can be seen that with the array perpendicular to the LOS the eigenvalues are more evenly distributed. This explains the larger capacity for this case. The eigenvalue distribution is of course also affected by the correlation of the transfer functions between the antenna elements. Since we have a strong LOS component the correlations are rather large. The transmit and receive complex correlation matrices for the two orientations are estimated, with a magnitude of the first column vector of

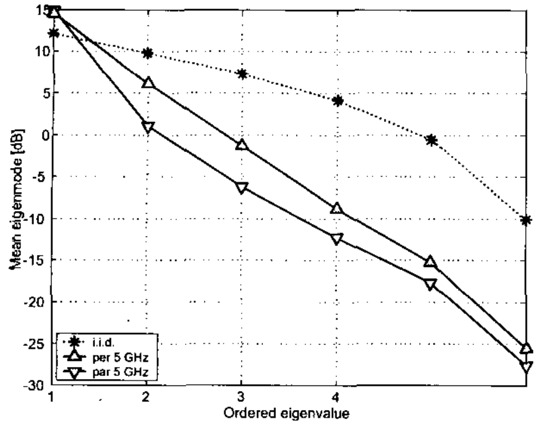

Fig. 3. Ordered eigenvalues.

$$\left|\mathbf{r}_R^{(\parallel)}\right| = \begin{bmatrix} 1 \\ 0.94 \\ 0.87 \\ 0.79 \\ 0.74 \\ 0.73 \end{bmatrix} \quad \left|\mathbf{r}_R^{(\perp)}\right| = \begin{bmatrix} 1 \\ 0.89 \\ 0.70 \\ 0.55 \\ 0.48 \\ 0.45 \end{bmatrix}, \qquad (5)$$

$$\left|\mathbf{r}_T^{(\parallel)}\right| = \begin{bmatrix} 1 \\ 0.86 \\ 0.69 \\ 0.56 \\ 0.51 \\ 0.52 \end{bmatrix} \quad \left|\mathbf{r}_T^{(\perp)}\right| = \begin{bmatrix} 1 \\ 0.87 \\ 0.68 \\ 0.55 \\ 0.51 \\ 0.51 \end{bmatrix}. \qquad (6)$$

As seen in (5) and (6), the receiver correlation is highest when the broadside of the receive array is parallel to the LOS, which also explains the large difference between the largest and second largest eigenvalues for this case. The transmit correlations are almost equal for the two orientations.

IV. Directions of Multipath Components

In order to get a better physical interpretation of the measurement results, and to form a basis for a physical model, we estimate the DOD and the DOA from the channel measurements. The 201 sub-channels measured over 500 MHz are inverse Fourier transformed to yield the impulse response. For each of the resulting time sample the 2D unitary ESPRIT algorithm [13] is used to find the corresponding DOD-DOA pairs. The source order i.e. the number of MPC to be estimated for each time sample, is required for the 2D unitary ESPRIT algorithm, and we estimate the source order with the maximum-description-length (MDL) algorithm [13]. A conventional beamformer estimates the power for each DOA and DOD pair.

In Fig. 4 the estimated MPCs down to -25 dB of the LOS component are plotted. The resolution of a linear array is higher in the boresight direction than in the endfire of the array,

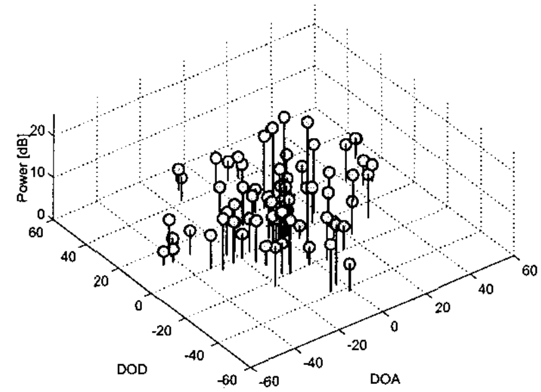

Fig. 4. Estimated DOD and DOA relative to LOS for the perpendicular orientation. MPC down to -25 dB of the dominant component are plotted.

thus the resolution of MPCs is higher in the perpendicular orientation and a lager number of MPC is found for this orientation.

A. Geometrical analysis

The estimated DOAs and DODs give us important insights into the propagation process, and their impact on the capacity. The capacity difference for the two considered array orientations can be explained by the following observations:

- Scatterers are placed on the opposite walls of the corridor with the same distance to the receiver array (we call them mirror scatterers) can not be distinguished with the orientation parallel to the LOS (see Fig. 1). Thus for this orientation, two scatterers placed at the same distance (single bounce) will not result in any additional spacial dimensions of the MIMO channel. The same mirrored scatters can be distinguished with the perpendicular orientation, and will therefore result in an additional channel capacity gain compared to the previous orientation.
- Channel capacity is highly dependent on the correlation between the receiver antenna elements (when no 'key-holes' are present [14]). The correlation between the elements is determined by the scatter environment and the ability of the array's to distinguish between scatters [4]. Hence, the number of scatters and their distribution (e.g. DOAs) will affect the channel capacity. A linear antenna array has a better angular resolution in directions perpendicular to the broadside of the array than for directions parallel to the broadside. Hence, in our narrow corridor, the perpendicular orientation has in average a larger number of scatters in the "high resolution area", compared to the parallel orientation. This results in a higher number of spatial degrees of freedom and lower correlation (5) and (6) for the perpendicular case.

V. Models

The properties of the MIMO cannel can be described both using physical models and using non-physical (statistical) models. In this section we compare the measured capacity results to capacity calculated by two such models.

A. Physical model

The signal transmitted on a wireless channel propagates along several paths, due to reflections and scattering from physical objects. Each of the K resolvable multipath component (MPC) is delayed in accordance to its excess-delay τ_k, and weighted with the proper complex amplitude $a_k e^{j\phi_k}$. Additionally, each DOD $\Omega_{T,k}$ is connected to the corresponding DOA $\Omega_{R,k}$. A stationary flat fading double directional channel complex impulse response between transmitter antenna element n at location $\vec{x}_{T,n}$ and receiver antenna element m at location $\vec{x}_{R,m}$, can be expressed as [8]

$$h_{m,n} = \sum_{k=1}^{K} h\left(\Omega_{R,k}, \Omega_{T,k}\right) \tag{7}$$
$$\times g_R\left(\Omega_R\right) g_T\left(\Omega_T\right) e^{j\frac{2\pi}{\lambda}\langle \vec{e}(\Omega_{R,k}), \vec{x}_{R,m}\rangle} e^{j\langle \vec{e}(\Omega_{T,k}), \vec{x}_{R,n}\rangle},$$

where $\vec{x}_{R,m}$ and $\vec{x}_{T,n}$ are the vectors of the chosen element-position measured from an arbitrary but fixed reference point on the corresponding array, and where

$$h\left(\Omega_{R,k}, \Omega_{T,k}\right) = \tag{8}$$
$$a_k e^{j\phi_k} \delta\left(\Omega_R - \Omega_{R,k}\right) \delta\left(\Omega_T - \Omega_{T,k}\right).$$

$\vec{e}(\Omega)$ denotes the unit pointing vector towards Ω in the horizontal plane, and

$$\langle \vec{e}(\Omega), \vec{x}\rangle = |x| \sin \Omega, \tag{9}$$

and λ is the wave length. Further, $g_R(\Omega_R)$ and $g_T(\Omega_T)$ are the antenna element gain responses in the receiver and transmitter. In our measurements we use omnidirectional antennas, thus $g_R(\Omega_R)$ and $g_T(\Omega_T)$ are equal to 1 for all Ω_R and Ω_T. Due to the small sub-channel bandwidth relative to the coherence bandwidth, the flat fading assumption results in the same excess delay, τ_k, for all MPCs. Since the channel is stationary the multipath parameters do not depend on the absolute time. The complex MIMO channel matrix for the flat fading channel could then be expressed as

$$\mathbf{H}_{\text{mod}} = \begin{bmatrix} h_{1,1} & \cdots & h_{1,N_T} \\ \vdots & \ddots & \vdots \\ h_{N_R,1} & \cdots & h_{N_R,N_T} \end{bmatrix}. \tag{10}$$

Based on this channel matrix we calculate the capacity.

B. Non-physical LOS model

In [15] the non-physical LOS channel model consists of two parts: a dominant part modelling the LOS component, $\mathbf{H}_{\text{LOS}}$, and a residual channel $\mathbf{H}_{\text{res}}$. The weighted sum then represents the LOS model as

$$\mathbf{H}_{\text{mod}} = (1-\alpha)\, \mathbf{H}_{\text{LOS}} + \alpha \mathbf{H}_{\text{res}}, \tag{11}$$

where $E\left[\|\mathbf{H}_{\text{LOS}}\|_F^2\right] = N_R N_T$ and $E\left[\|\mathbf{H}_{\text{Res}}\|_F^2\right] = N_R N_T$. The residual channel matrix is found by projecting the measured data to the null-space, $\mathbf{H}_{\text{res}}(m) = \mathbf{\Pi}^{\perp}(m)\, \mathbf{H}(m)$, of the estimated LOS DOA, which is done for each measured sub-channel. With the LOS array steering vector defined as

$$\mathbf{a}(\Omega) = \left[\begin{array}{ccc} e^{-j\pi \sin(\Omega)} & \cdots & e^{-j\pi N_R \sin(\Omega)} \end{array}\right], \tag{12}$$

the null space becomes

$$\mathbf{\Pi}^{\perp} = \mathbf{I} - \frac{\mathbf{a}\left(\Omega_{R,\text{LOS}}\right) \mathbf{a}^H\left(\Omega_{T,\text{LOS}}\right)}{\mathbf{a}^H\left(\Omega_{R,\text{LOS}}\right) \mathbf{a}\left(\Omega_{T,\text{LOS}}\right)}. \tag{13}$$

Without the dominant path the residual channel is assumed to have a Rayleigh distribution and its covariance matrix can then be approximated by the Kronecker product. The residual channel is now described by

$$\hat{\mathbf{H}}_{\text{res}} = \left(\hat{\mathbf{R}}_R\right)^{1/2} \mathbf{G} \left(\hat{\mathbf{R}}_T\right)^{T/2}, \tag{14}$$

where $\mathbf{G}$ is a stochastic matrix with complex Gaussian i.i.d. entries, $(\cdot)^{1/2}$ is matrix square root defined as $\mathbf{A}^{1/2}\left(\mathbf{A}^{1/2}\right)^{\dagger} = \mathbf{A}$. The covariance matrices are estimated as

$$\hat{\mathbf{R}}_T = \frac{1}{M N_T} \sum_{m=1}^{M} \left(\mathbf{H}_{\text{res}}^{\dagger}(m)\, \mathbf{H}_{\text{res}}(m)\right)^T, \tag{15}$$

$$\hat{\mathbf{R}}_R = \frac{1}{M N_R} \sum_{m=1}^{M} \mathbf{H}_{\text{res}}(m)\, \mathbf{H}_{\text{res}}^{\dagger}(m). \tag{16}$$

The channel matrix is now modelled as the weighted sum of the rank one LOS matrix and residual channel matrix

$$\hat{\mathbf{H}}_{\text{mod}} = \tag{17}$$
$$(1-\alpha)\, \mathbf{a}\left(\Omega_{R,\text{LOS}}\right) \left(\mathbf{a}\left(\Omega_{T,\text{LOS}}\right)\right)^T + \alpha \left(\hat{\mathbf{R}}_R\right)^{1/2} \mathbf{G} \left(\hat{\mathbf{R}}_T\right)^{T/2},$$

where the weighting factor α is the defined as

$$\alpha = \sqrt{\frac{1}{M N_R N_T} \sum_{m=1}^{M} \|\mathbf{\Pi}^{\perp}(m)\, \mathbf{H}(m)\|_F^2}. \tag{18}$$

C. Comparison of model and measurement

In Fig. 5 the measured capacities and the expected capacities calculated for the two models are shown. It can seen that the two channel models are able to identify the effect of the horizontal orientation. The agreements with the measured capacities are however not that precise, especially not for the perpendicular orientation. The physical model is highly dependent of the angular estimates and the corresponding power estimates. The performance of the 2D unitary ESPRIT gets worse with the decrease in angular separation between MPCs [13]. Since a major part of the strong MPCs arrives with a small angle separation due to the 'wave-guiding' effect of the corridor we might have a poor angular estimate for some MPCs. The estimation uncertainties together with unresolved MPCs may results in the discrepancy of the physical model.

The projection to the null space of the LOS direction for the non-physical model removes not only the LOS component but also reflected MPC arriving in the LOS direction to the

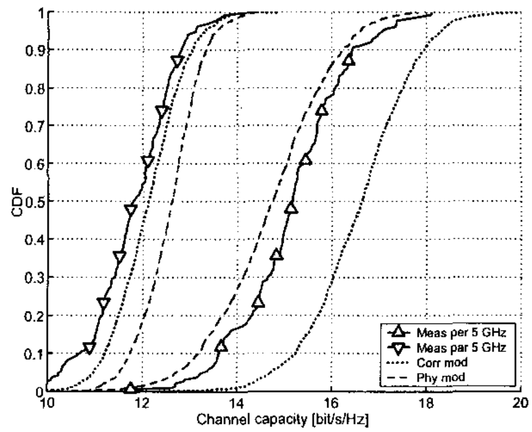

Fig. 5. Physical and non-physical model capacity comparison with the measured channel for $N_R = N_T = 6$.

receiver array. MPC with a DOA close to the LOS component are significantly attenuated by the projection to the LOS's null space. This might result in an underestimated correlation for the residual channel and therefor an overestimated capacity.

VI. Conclusions

In this paper an analysis of the impact of receiver antenna horizontal orientation on the channel capacity of a 6×6 MIMO system was presented. It has been shown that in a 'wave guiding' environment such as a long corridor with the presence of a strong LOS, a significant difference in capacity is observed when the linear receiver array orientation is changed from parallel to perpendicular (to the LOS). An independent measurement campain was performed in a subway tunnel [16], presenting similar results. For the corridor under investigation, the perpendicular receiver array allows additional spatial dimensions of the MIMO channel by distinguishing between those scatters on the opposite walls of the corridor with the same distance to the receiver array. The parallel array would be unable to distinguish between these 'mirrored' scatters and hence capacity gain for this orientation is significantly lower. The complex spatial correlation was estimated and the parallel orientation shows a higher correlation between the receiver antenna elements compared to the perpendicular orientation.

Acknowledgement: We would like to thank Dr. Pejman Hafezi for his helpful comments and advice. Part of this work was financed by an INGVAR grant of the Swedish Strategic Research Foundation.

References

[1] J. H. Winters, "On the capacity of radio communications systems with diversity in Rayleigh fading environments," *IEEE Journal on Selected Areas in Communications*, vol. 5, pp. 871–878, June 1987.

[2] G. J. Foschini and M. J. Gans, "On limits of wireless communications in fading environments when using multiple antennas," *Wireless Personal Communications*, vol. 6, pp. 311–335, 1998.

[3] I. E. Telatar, "Capacity of multi-antenna gaussian channels," *European Transactions on Telecommunications*, vol. 10, November–December 1999.

[4] D. Shiu, G. J. Foschini, M. J. Gans, and J. M. Kahn, "Fading correlation and its effect on the capacity of multi-element antenna systems," *IEEE Transactions on Communications*, vol. 48, pp. 502–513, March 2000.

[5] D. Hampicke, C. Schneider, M. Landmann, A. Richter, G. Sommerkorn, and R. S. Thoma, "Measurement-based simulation of mobile radio channels with multiple antennas using a directional parametric data model," in *Proc. VTC 2001 Fall*. 2001, vol. 2, pp. 1073–1077, IEEE.

[6] J. P. Kermoal, L. Schumacher, P. E. Mogensen, and K. I. Pedersen, "Experimental investigation of correlation properties of MIMO radio channels for indoor picocell scenarios," in *VTS Fall 2000*. April 2000, vol. 1, pp. 14–21, IEEE.

[7] M. J. Gans, N. Amitay, Y. S. Yeh, Xu Hao, T. C. Damen, R. A. Valenzuela, and T. Sizer, "Outdoor blast measurement system at 2.44 GHz: calibration and initial results," *IEEE Journal on Selected Areas in Communications*, vol. 20, pp. 570–583, 2002.

[8] A. F. Molisch, M. Steinbauer, M. Toeltsch, E. Bonek, and R. S. Thoma, "Capacity of MIMO systems based on measured wireless channels," *IEEE Journal on Selected Areas in Communications*, vol. 20, pp. 561–569, April 2002.

[9] P. Kyritsi, "Correlation measures for MIMO systems," in *COST 273*, May 2002, p. TD(02) 037.

[10] T. M. Cover and J. A. Thomas, *Elements of Information Thoery*, Wiley, 1991.

[11] P. Almers, F. Tufvesson, O. Edfors, and A. F. Molisch, "Measured capacity gain using waterfilling in frequency selective MIMO channels," in *Proc. PIMRC*. 2002, IEEE.

[12] P. F. Driessen and G. J. Foschini, "On the capacity formula for multiple input-multiple output wireless channels: A geometric interpretation," *IEEE Transactions on Communications*, vol. 47, pp. 173–176, 1999.

[13] M. Haardt, *Efficient One-, Two-, and Multidimensional High-Resolution Array Signal Processing*, Ph.D. thesis, München Technical University, Germany, 1997.

[14] D. Chizhik, G. J. Foschini, M. J. Gans, and R. A. Valenzuela, "Keyholes, correlations, and capacities of multielement transmit and receive antennas," *IEEE Transactions on Communications*, vol. 1, pp. 361–368, April 2002.

[15] K. Yu, "Modeling of multiple-input multiple-output radio propagation channels," Licentiate Thesis, July 2002, KTH, Sweden.

[16] M. Lienard, P. Degaunque, D. Degardin, and J. Baudet, "Theoretical and experimental analysis of the channel capacity enhancement based on MIMO techniques in subway tunnels," in *PIMRC 2002*, Lisboa, 2002, IEEE.